

**Homework 2 - Solution**

**Problem 1: Capillary rise/fall in cylindrical tubes**

**A. Capillary rise in PVC tubes**

We know the meniscus in the tube will take a spherical shape; the radius of this sphere is (Figure 1):

$$R_A = \frac{r_i}{\cos \theta}$$

The liquid pressure right underneath the meniscus  $P_1$  should satisfy the Young-Laplace equation. In this case as  $P_{atm}$  is larger than  $P_1$ , the phase *I* of the Y-L equation is the air and the phase *II* is the liquid, we obtain:

$$P_{atm} - P_1 = \frac{2\gamma}{R_A} = \frac{2\gamma}{r_i} \cos \theta$$

At the base surface of the liquid pool, location 2, the surface is flat,

$$P_2 - P_{atm} = 0$$

Due to the hydrostatic pressure,

$$P_2 - P_1 = \rho g z_i$$

Thus,

$$\frac{2\gamma}{r_i} \cos \theta = \rho g z_i$$

We obtain the expression of the capillary rise:

$$z_i = \frac{2\gamma \cos \theta}{r_i \rho g}$$

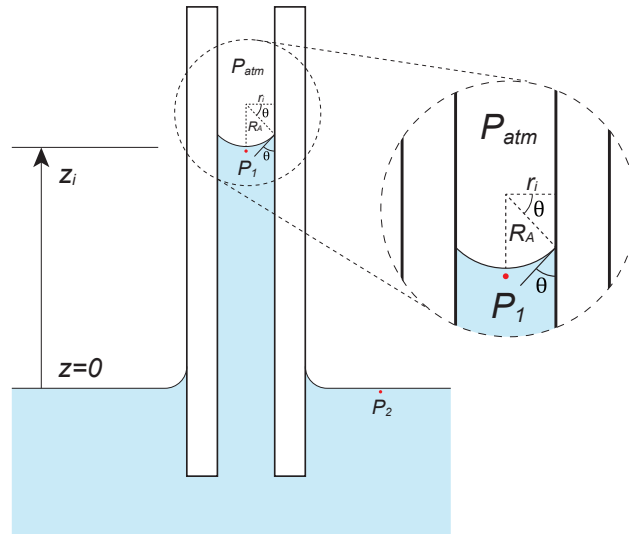


Figure 1: Capillary rise in PVC tube

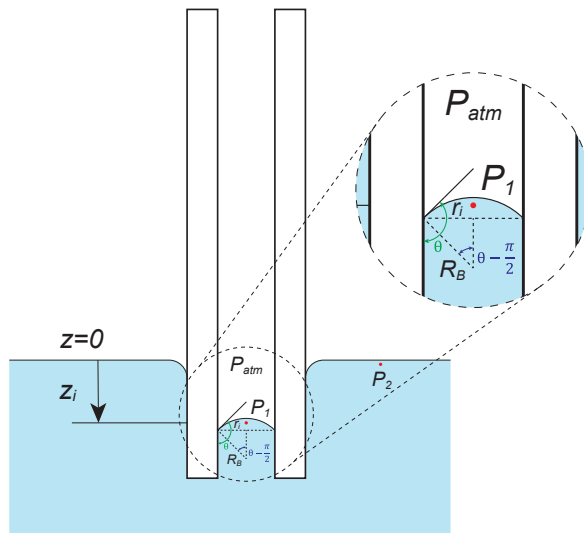


Figure 2: Capillary fall in Teflon tube

---

## B. Capillary fall in Teflon tubes

In the hydrophobic case  $\cos \theta > \pi/2$ . The radius of curvature for the spherical meniscus in the tube is (Figure 2) :

$$R_B = \frac{r_i}{\sin(\theta - \frac{\pi}{2})} = \frac{r_i}{-\cos \theta} > 0$$

The pressure right underneath the meniscus  $P_1$ , satisfies the Young-Laplace equation. This time, phase *I* is the liquid, and phase *II* is the air as the pressure in the liquid is higher than the atmospheric pressure, we obtain:

$$P_1 - P_{atm} = \frac{2\gamma}{R_B} = -\frac{2\gamma}{r_i} \cos \theta$$

Similar to case A, we have  $P_2 = P_{atm}$ , but the hydrostatic part is different:

$$P_1 - P_2 = \rho g z_i$$

Thus,

$$-\frac{2\gamma}{r_i} \cos \theta = \rho g z_i$$

We obtain the expression of the capillary fall:

$$z_i = -\frac{2\gamma \cos \theta}{r_i \rho g}$$

---

## Problem 2: Advancing/Receding droplet

### A. Advancement into the non-wetting material

For a virtual advancement of the contact line on the non-wetting material (Figure 3a), the solid-liquid interfacial energy is increased by

$$\Delta A \cdot \sigma_{ls_2}$$

The solid-vapor interfacial energy is decreased by

$$\Delta A \cdot \sigma_{vs_2}$$

And, the liquid-vapor interfacial energy is increased by

$$\Delta A \cdot \sigma_{lv} \cos \theta$$

The total energy increase is

$$\Delta E_{adv} = \Delta A(\sigma_{ls_2} - \sigma_{vs_2} + \sigma_{lv} \cos \theta)$$

Young's equation on a flat surface made of Material 2 gives us

$$\sigma_{ls_2} - \sigma_{vs_2} + \sigma_{lv} \cos 120^\circ = 0$$

So, if  $\theta < 120^\circ$ ,  $\Delta E_{adv} > 0$

Therefore, on the principle of energy minimization, the advancement won't spontaneously occur.

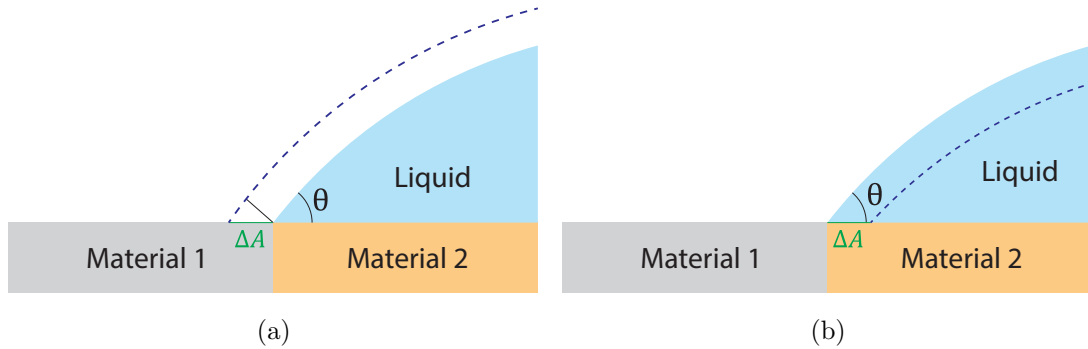


Figure 3: (a) Advancement into the non-wetting material. (b) Receding into the wetting material.

---

## B. Receding into the wetting material

In the receding case (Figure 3b), the net energy increase is

$$\Delta E_{rec} = \Delta A(\sigma_{vs_1} - \sigma_{ls_1} - \sigma_{lv} \cos \theta)$$

Young's equation on a flat surface made of Material 1 gives us

$$\sigma_{vs_1} - \sigma_{ls_1} - \sigma_{lv} \cos 30^\circ = 0$$

So if  $\theta > 30^\circ$ ,  $\Delta E_{rec} > 0$ .

Therefore, no receding will spontaneously occur.

### Problem 3: Micropillared surface

We need first to identify some key parameters of the structured substrate:

Top surface solid fraction:

$$\phi = \frac{a^2}{(a+b)^2} = \frac{1}{9}$$

Roughness ratio:

$$r = \frac{4ah + (a+b)^2}{(a+b)^2} = \frac{17}{9}$$

Critical penetration angle

$$\theta_c = \arccos\left(\frac{1-\phi}{r-\phi}\right) = \frac{\pi}{3} \text{ or } 60^\circ$$

The rest can be done by following the different regimes covered in the lecture (Hemi-spearling state, Wenzel state, and Cassie-Baxter state). A map summarizing the different regimes is shown in Figure 4 with the specific equations to be used.

Since we asked to plot in terms of angles, not the cosine, the plot should be similar to the Figure 5. Pay special attention to the transition at  $60^\circ$  and  $90^\circ$  for  $\theta_Y$ .

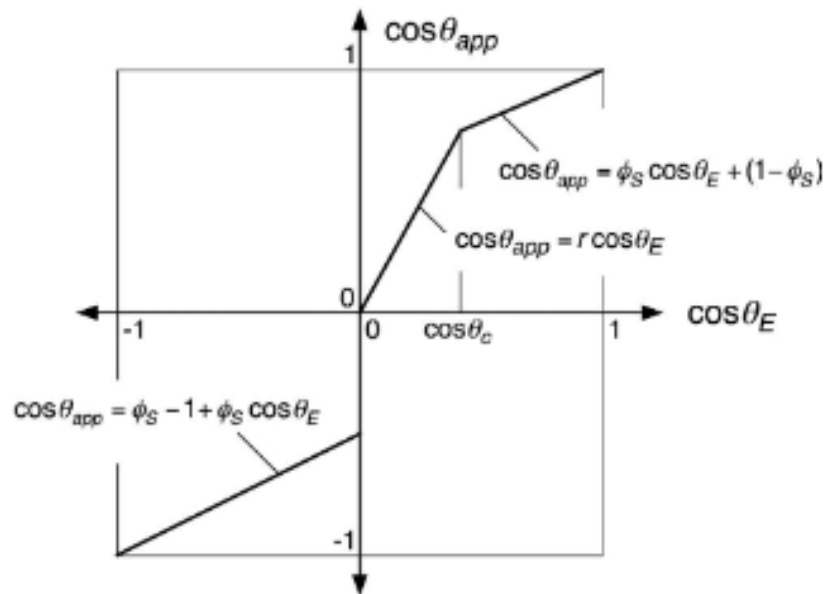


Figure 4: Different regimes (Figure 3.24 in Carey)

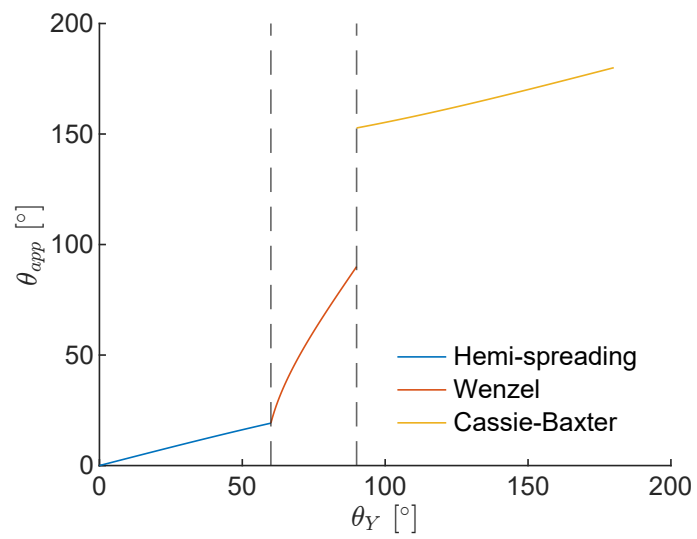


Figure 5: Plot of the apparent contact angle  $\theta_{app}$  as a function of the intrinsic Young's contact angle  $\theta_Y$